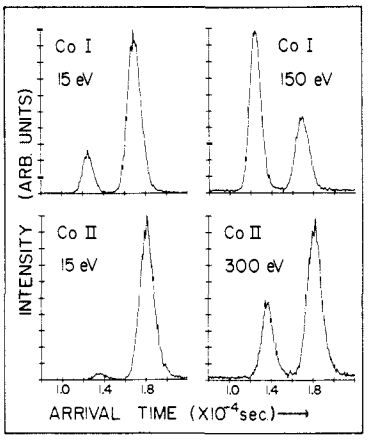

Figure 1. Arrival-time distribution of Co^+ in He; $P_{He} \simeq 1.0$ Torr, $T = 160$ K for $CoCO_3NO$ (I) and $CoCp(CO)_2$ (II). The shift in arrival time between I and II is due to slightly different E/N values in the experiments. The times shown include time in the quadrupole, which must be subtracted to determine the mobility.

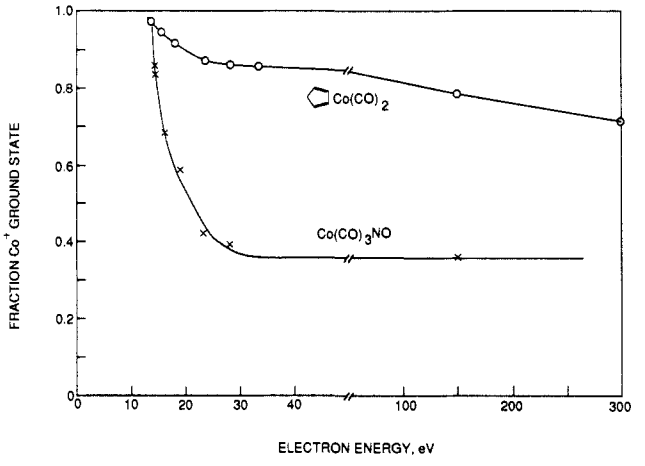

Figure 2. Percent Co^+ ground state versus ionizing energy. Note change in energy axis at 50 eV.

distribution of times between injection and collection forms the arrival-time distribution. Total time between ion formation and collection is 100–400 μs. No ions other than Co^+ and $Co{\cdot}He^+$ ($\lesssim$1%) were observed after the reaction cell.

Figure 1 shows the ATDs for Co^+ formed from I and II. In both cases, two peaks are observed and the peak at longer time (lower mobility) increases with decreasing ionizing energy, approaching 100% at ~14 eV. Figure 2 shows the percent slower peak versus ionizing energy. An unlikely explanation is the formation of another ion with the same nominal mass which could not be differentiated in the quadrupole. The m/e 59 peak was examined at high resolution, and no such ion was found. We are convinced that the peaks are due to ground-state $Co^+(3d^8,{}^3F)$ and a metastable excited state, probably $Co^+(3d^74s^1,{}^3F)$. The respective zero field reduced mobilities[12] were measured to be $K_0 = 16.2 \pm 2$ cm^2/(V s) (ground state) and $K_0 = 24.1 \pm 2$ cm^2/(V s) (excited state); their ratio is 1.485 ±0.05. No variation in K_0 was found between cell temperatures of 160 and 300 K.

If Co^+ electronic states are responsible for the different mobilities, the increased mobility of the ^3F state is probably due to the populated 4s orbital. The 4s orbital is considerably larger than the 3d;[2,13] thus, long-range repulsion between Co^+ and He should increase if it is occupied. This will reduce the effective attractive potential due to the charge-induced dipole, lowering the collision rate. Tonkyn et al.[2] have used this argument to help explain metal ion/alkane clustering data. Mobilities in helium are often determined largely by forces other than the charge-induced dipole, due to the small polarizability of helium.[12,14] The existing Ti^+ mobility data[9] support the above hypothesis. The Ti^+ ground state ($3d^24s^1,{}^4F$) includes a 4s electron[6] and has a mobility of 25.5 ± 0.5 cm^2/(V s),[9] very similar to that of the excited-state cobalt. This may indicate that configuration (not electronic state) determines mobility. Further support for long-range repulsion between excited Co^+ and He comes from the absence of deactivation in collisions with helium ($k < 1 \times 10^{-14}$ cm^3/s). Deactivation might be expected in an intimate collision. We are examining other first-row transition metals to check the correlation between high mobility and occupied 4s orbital.

Finally, we can compare the apparent effects of 3d and 4s orbital population on ion mobility. Potassium ions ($3p^6,{}^1S$) have a mobility of He of 21.6 cm^2/(V s).[14,15] If the metal ion/He interaction were purely electrostatic (i.e., charge-induced-dipole attraction versus electron–electron repulsion), we would expect that adding 3d electrons to K^+ should cause some increase in mobility due to increased electron density on the ion while adding a 4s electron should cause a greater increase.[16] In fact, the 3d electrons cause a large *decrease* in mobility (at least for ground-state Co^+), indicating a decreased repulsion, which must be due to other factors. Studies of other first row transition metal ions are in progress.

Acknowledgment. National Science Foundation support under Grant CHE88-17201 is gratefully acknowledged.

(12) McDaniel, E. W.; Mason, E. A. *The Mobility and Diffusion of Ions in Gases*; Wiley: New York, 1973; p 6.
(13) Huheey, J. E. *Inorganic Chemistry*; Harper and Row: New York, 1972; pp 40–43.
(14) Lindinger, W.; Albritton, D. L. *J. Chem. Phys.* **1975**, *62*, 3517.
(15) Ellis, H. W.; et seqq. Transport Properties of Gaseous Ions Over a Wide Range. *At. Nucl. Data Tables* **1976**, *17*, 177; **1978**, *22*, 179; **1984**, *31*, 113.
(16) Electron density at 2.5 Å in Co^+ increases by 7.5 when a 4s electron is added (see ref 2).

Structural Studies by $^1H/^{13}C$ Two-Dimensional and Three-Dimensional HMQC–NOE at Natural Abundance on Complex Carbohydrates

P. de Waard, R. Boelens,* G. W. Vuister, and J. F. G. Vliegenthart

Department of Chemistry, University of Utrecht Padualaan 8, 3584 CH Utrecht, The Netherlands

Received October 3, 1989

Studies on the chain conformation of oligosaccharides are mainly restricted to analysis of NOE spectra to estimate the torsion angles defining the glycosidic linkages.[1,2] A major problem in the analysis is the overlap of resonances in the bulk region between 3 and 4 ppm. Recently, we demonstrated a homonuclear 3D NOE–HOHAHA experiment to resolve overlap in 2D NOE spectra of oligosaccharides.[3] ^{13}C spectra of oligosaccharides are much better resolved than ^1H spectra. Therefore, the inclusion or addition of a ^{13}C frequency domain is a promising extension of 2D ^1H NOE spectroscopy. So far heteronuclear NMR experiments such as 2D and 3D HMQC–NOE have been limited to isotope-enriched proteins.[4-9] Furthermore, $^1H/^{13}C$ HMQC–

(1) Carver, J. P.; Brisson, J. R. *Biology of Carbohydrates*; Wiley: New York, 1984; pp 289–331.
(2) Homans, S. W.; Dwek, R. A.; Rademacher, T. W. *Biochemistry* **1987**, *26*, 6571–6578.
(3) Vuister, G. W.; De Waard, P.; Boelens, R.; Vliegenthart, J. F. G.; Kaptein, R. *J. Am. Chem. Soc.* **1989**, *111*, 772–774.
(4) Fesik, S. W.; Zuiderweg, E. R. P. *J. Magn. Reson.* **1988**, *78*, 588–593.
(5) Fesik, S. W.; Luly, J. R.; Erickson, J. W.; Abad-Zapatero, C. *Biochemistry* **1988**, *27*, 8297–8301.
(6) Shon, K.; Opella, S. J. *J. Magn. Reson.* **1989**, *82*, 193–197.
(7) Marion, D.; Kay, L. E.; Sparks, S. W.; Torchia, D. A.; Bax, A. *J. Am. Chem. Soc.* **1989**, *111*, 1515–1517.

0002-7863/90/1512-3232$02.50/0

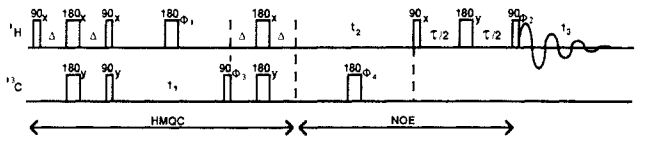

Figure 1. Pulse sequence of 3D HMQC-NOE. The following phase cycling is used: $\Phi_1 = 2(x,x,-x,-x,y,y,-y,-y)$; $\Phi_2 = 8(x)$, $8(-x)$; $\Phi_3 = 8(x,-x)$; $\Phi_4 = 4(x,-x,-x,x)$; acq = $2(x,-x)$, $4(-x,x)$, $2(x,-x)$. Positive and negative frequencies in ω_1 and ω_2 were separated by independent TPPI on the 90° ^{13}C pulse for ω_1 and all pulses prior to the t_2 evolution period for ω_2. The delay Δ is equal to $1/(4J(^1H-^{13}C))$; the delay τ is the NOE mixing period. The extra delays Δ after the evolution period will refocus antiphase magnetization into in-phase magnetization before starting the NOE part. The ^1H and ^{13}C 180° pulses are repeated during this delay to be able to phase the spectrum afterwards. ^{13}C decoupling in the t_2 evolution period is accomplished by a ^{13}C 180° pulse in the center of t_2.

COSY and HMQC–HOHAHA have been performed.[10-13] Here we give an example of the application of $^1H/^{13}C$ HMQC-NOE at natural abundance to the diantennery asparagine-linked oligosaccharide **1** as a tool for structural analysis.

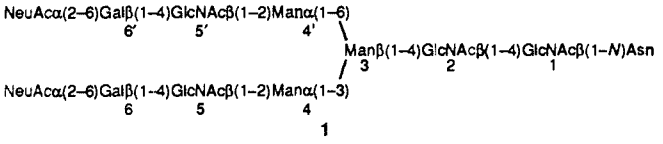

A 3D HMQC-NOE experiment can be regarded as a combination of a 2D HMQC and a 2D NOE experiment (Figure 1). The HMQC part, containing an effective suppression of ^{12}C magnetization terms, is essentially as used before.[14-16] The excitation of ^{12}C z magnetization during the NOE part can be effectively suppressed by using a $90°_x-\tau/2-180°_y-\tau/2-90°_x$ mixing sequence. ^{13}C decoupling in the acquisition period is not necessary. The NOE magnetization exchange involves mainly transfer from a proton attached to ^{13}C to a proton attached to ^{12}C; by consequence, NOE cross peaks ($\omega_2 \neq \omega_3$) are not split by the $^1H-^{13}C$ coupling. Only cross peaks containing magnetization not transferred during the NOE period ($\omega_2 = \omega_3$) will be split by the $^1H-^{13}C$ coupling in the ω_3 domain. These HMQC cross peaks are found on the diagonal ($\omega_2 = \omega_3$) of a cross-sectional plane perpendicular to the ω_1 axis. NOEs are found on a line perpendicular to the ω_2 axis. The absence of decoupling yielded a more stable measurement.

In Figure 2, three ω_1 cross sections of the 3D HMQC-NOE spectrum of **1** are shown. The small number of 112 increments in the ^{13}C t_1 direction results in a poor resolution; therefore, both GlcNAc-5/5′ H-1 (δ C-1 = 100.6 ppm) and Man-4 H-1 (δ C-1 = 100.8 ppm) are present on the diagonal (Figure 2A). Comparison with a 2D NOE spectrum (insert) demonstrates that the HMQC sequence has selected a small part of the 2D NOE spectrum. The NOE effect between Man-3 H-3 and Man-4 H-1 cannot be unambiguously identified in 2D NOE nor in the homonuclear 3D NOE–HOHAHA experiment[3] because of overlap with Man-4 H-5 (see Figure 2A). In 3D HMQC-NOE (Figure 2B), this NOE is not disturbed by overlap. The ω_1 cross section at ω_1 = 70 ppm of NeuAc H-7 and H-4 and Gal H-4 shows an

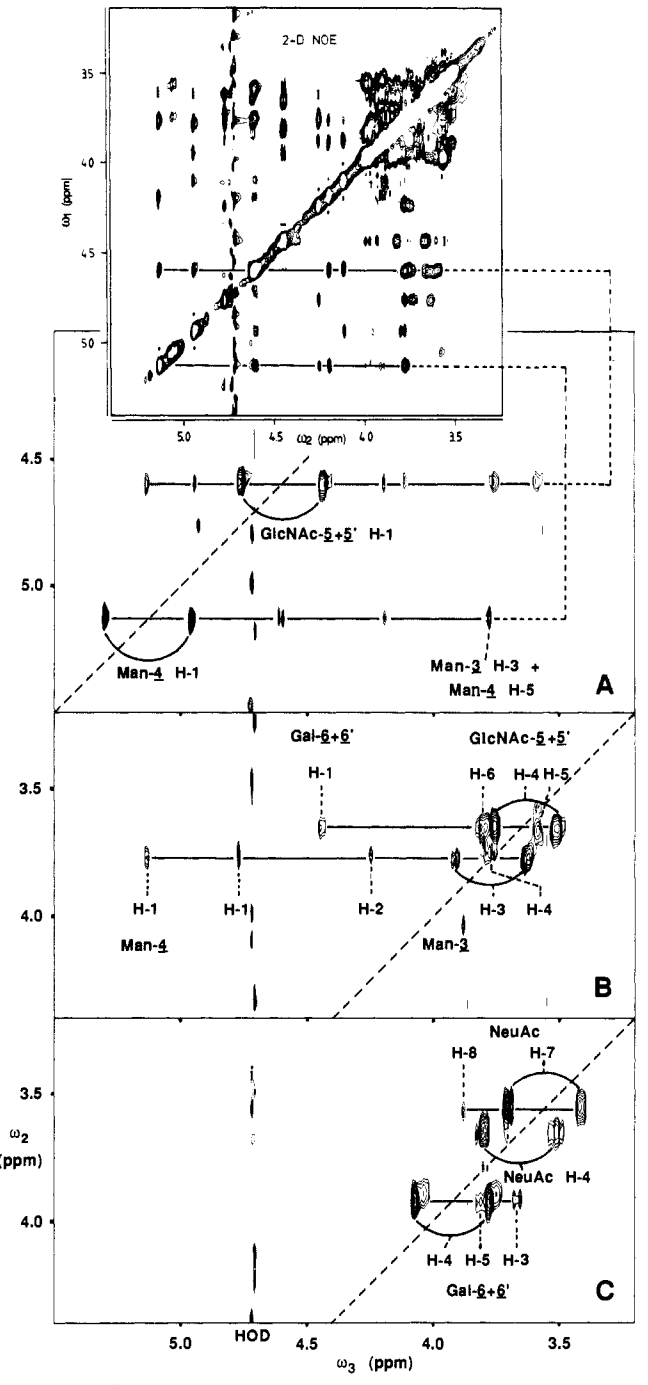

Figure 2. Cross sections perpendicular to the ω_1 axis of the 3D HMQC-NOE $^1H/^{13}C$ spectrum of a 20 mM solution of **1** in D_2O at 304 K and pH 7. Cross sections are shown at ω_1 frequencies of 101 ppm (A), 82 ppm (B), and 70 ppm (C). The phase-sensitive spectrum was recorded at 500 MHz on a Bruker AM500 spectrometer. Acquisition was preceded by four dummy scans. FIDs of 16 scans were recorded at a size of 1K. This was repeated independently for 112 incremental t_1 and 96 incremental t_2 values, resulting in a total measuring time of approximately 63 h. The relaxation delay was 0.6 s; Δ was 1.78 ms. Spectral width in the ^1H time domains was 2272.7 Hz and, in the ^{13}C time domain, 11 364 Hz. The NOE mixing time was 0.35 s. Data were zero-filled twice in the t_1 and t_2 domains before Fourier transformation. A cosine window multiplication was used in the t_3 domain, while a Hamming window was used in the t_2 and t_1 domains.[17] The resulting data set of 256 × 256 × 512 points was base-line-corrected in all frequency domains by a fourth-order polynomial fit.

example of NOEs between protons resonating within the bulk region (Figure 2C). The NOE between NeuAc H-7 and H-8 is of importance to determine the conformation of the glycerol side chain of NeuAc. This NOE cannot be identified in the homonuclear 3D NOE–HOHAHA spectrum, since the small coupling

(8) Zuiderweg, E. R. P.; Fesik, S. W. *Biochemistry* **1989**, *28*, 2387–2391.
(9) Fesik, S. W.; Gampe, R. T., Jr.; Zuiderweg, E. R. P.; Kohlbrenner, W. E.; Weigl, D. *Biochem. Biophys. Res. Commun.* **1989**, *159*, 842–847.
(10) Lerner, L.; Bax, A. *J. Magn. Reson.* **1986**, *69*, 375–380.
(11) Wagner, G.; Brühwiler, D. *Biochemistry* **1986**, *25*, 5839–5843.
(12) Fesik, S. W.; Gampe, R. T., Jr.; Zuiderweg, E. R. P. *J. Am. Chem. Soc.* **1989**, *111*, 770–772.
(13) Davis, D. G. *J. Magn. Reson.* **1989**, *84*, 417–424.
(14) Müller, L. *J. Am. Chem. Soc.* **1979**, *101*, 4481–4484.
(15) Brühwiler, D.; Wagner, G. *J. Magn. Reson.* **1986**, *69*, 546–551.
(16) Otting, G.; Wütrich, K. *J. Magn. Reson.* **1988**, *76*, 569–574.
(17) Ernst, R. R.; Bodenhausen, G.; Wokaun, A *Principles of Nuclear Magnetic Resonance in One and Two Dimensions*; Clarendon: Oxford, 1987; p 103.

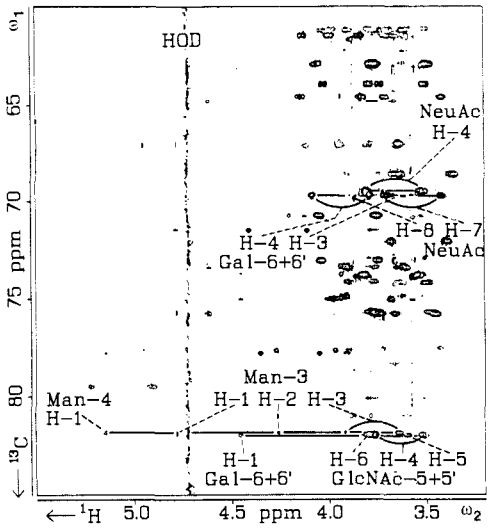

Figure 3. The bulk region of a 2D HMQC-NOE $^1H/^{13}C$ spectrum of a 20 mM solution of **1** in D_2O at 304 K and pH 7. The phase-sensitive spectrum was recorded at 500 MHz on a Bruker AM500 spectrometer. Acquisition was preceded by four dummy scans; 2048 t_1 increments of 48 scans each were recorded at a size of 2 K, resulting in a total measuring time of approximately 60 h. The relaxation delay was 1.0 s; Δ was 1.78 ms. Spectral width in the ^1H time domains was 2272.7 Hz and, in the ^{13}C time domain, 11 364 Hz. The NOE mixing time was 0.35 s. Cosine multiplications were used in the t_2 and t_1 domains. The resulting data set after Fourier transformation of 1024 × 1024 points was baseline-corrected in both frequency domains by a fourth-order polynomial fit.

between NeuAc H-6 and H-7 prevents magnetization transfer by the isotropic mixing to the well-resolved NeuAc H-3 protons.

The extra ^1H dimension t_2 will separate protons attached to carbon atoms having the same ^{13}C chemical shift. If there is no overlap in the ^{13}C spectrum, this extra dimension is not necessary. The pulse sequence of 2D HMQC-NOE is identical with the 3D sequence except that the evolution period t_2 and the decoupling pulse have been left out. Most NOEs found in the 3D spectrum of **1** are also identified in the 2D spectrum of **1** (Figure 3). NOEs as discussed for the 3D spectrum in Figure 2, parts B and C, are indicated in Figure 3. For compounds with a well-resolved ^{13}C spectrum, the 2D HMQC-NOESY sequence is a good alternative for the 3D sequence. For the majority of NOEs in the 3D spectrum of **1**, the third dimension is only needed to compensate for the poor resolution in the ^{13}C direction as is shown for the GlcNAc-5/5′ H-4 and Man-3 H-3 in Figure 2B. With the higher resolution of the 2D HMQC-NOE (2048 t_1 increments) as compared to the 3D experiment (112 t_1 increments), the ^{13}C frequencies of GlcNAc-5/5′ C-4 and Man-3 C-3 are now resolved (Figure 3). The NOE between Gal-6 H-4 and Gal-6 H-5 as indicated in Figure 2C is an example of a cross peak, which cannot be identified in the 2D spectrum due to overlap of the ^{13}C frequencies of Gal-6 C-4, NeuAc C-4, and NeuAc C-7. Here the extra ^1H dimension is needed to resolve the overlap by using the difference in ^1H chemical shift of Gal-6 H-4, NeuAc H-4, and NeuAc H-7 (Figure 2C).

The present work illustrates the usefulness of heteronuclear 2D and 3D NMR techniques in structure elucidations of complex oligosaccharides. Although the spectra shown are recorded at natural abundance, the sensitivity is sufficient to identify most of the NOEs of **1**. Editing 2D NOE with respect to the carbon frequency gives a key to elucidating NOEs of any proton hidden in the bulk region.

Acknowledgment. This work was supported by the Netherlands Foundation for Chemical Research (SON) with financial aid of the Netherlands Foundation of Scientific Research (NWO).

Thanks to Profs. G. Spik and J. Montreuil, Université des Sciences et Techniques de Lille Flandres Artois, France, for the gift of the diantennery compound.

Mechanism of the C–C Cleavage of Acetone by the Ruthenium Benzyne Complex $(PMe_3)_4Ru(\eta^2\text{-}C_6H_4)$: Formation and Reactivity of an Oxametallacyclobutane Complex

John F. Hartwig, Robert G. Bergman,* and Richard A. Andersen*

Department of Chemistry, University of California, and Materials and Chemical Sciences Division Lawrence Berkeley Laboratory 1 Cyclotron Road, Berkeley, California 94720

Received October 23, 1989

The reaction of acetone with the ruthenium benzyne complex $(PMe_3)_4Ru(\eta^2\text{-}C_6H_4)$ (**1**) results in cleavage of a C–C bond[1] in the ketone, leading to methane and **2**, an ortho-metalated enolate complex of acetophenone (Scheme I).[2] We now report the generation and spectroscopic characterization of a potential intermediate in this reaction: complex **3**, a rare example of an oxametallacyclobutane. This material is formed in an unusual transformation that involves overall β-migration of a phenyl group from ruthenium to carbon in a transition-metal enolate, followed by an apparent β-alkyl elimination reaction.[1f,g] Studies of the chemistry of complex **3** show that it undergoes a number of novel reactions, including several that involve fragmentation to α-methylstyrene.

The synthesis of oxametallacyclobutane complex **3** is shown in Scheme I. Solutions of enolate **5**, the expected product from the reaction of acetone with $(PMe_3)_4Ru(\eta^2\text{-}C_6H_4)$ (**1**), were prepared by treatment of benzyne complex **1** with Me_3NHCl (leading to *cis*- and trans-phenylchlororuthenium complexes **4**), followed by reaction with the potassium enolate of acetone.[3] Only the O-bound isomer was detected by ^1H and $^{31}P\{^1H\}$ NMR spectrometry at −20 °C, in contrast to most late-transition-metal enolates, which exist as the C-bound isomer.[4] At room temperature over the course of an hour, complex **5** rearranges by an intramolecular migration of the phenyl group to the unsaturated enolate substituent, to form oxametallacyclobutane complex **3**.[5,6]

Complex **3** exhibits a temperature-dependent ^1H NMR spectrum, presumably due to rapid, reversible dissociation of phosphine. Decomposition of **3**, due to irreversible dissociation of phosphine

(1) For other examples of C–C activation reactions, see: (a) Suggs, J. W.; Cox, S. D. *J. Organomet. Chem.* **1981**, *221*, 199. (b) Suggs, J. W.; Jun, C.-H. *J. Am. Chem. Soc.* **1984**, *106*, 3054. (c) Suggs J. W.; Wovkulich, M. J. *Organometallics* **1985**, *4*, 1101. (d) Suggs, J. W.; Jun, C.-H. *J. Am. Chem. Soc.* **1986**, *108*, 4679. (e) Crabtree, R. H. *Chem. Rev.* **1985**, *85*, 245. (f) Crabtree, R. H.; Dion, R. P.; Gibbone, D. J.; McGrath, D. V.; Holt, E. M. *J. Am. Chem. Soc.* **1986**, *108*, 7222 and references therein. (g) Watson, P. L.; Roe, D. C. *J. Am. Chem. Soc.* **1982**, *104*, 6471. (h) Bunel, E.; Berger, B. J.; Bercaw, J. E. *J. Am. Chem. Soc.* **1988**, *110*, 976.

(2) Hartwig, J. F.; Andersen, R. A.; Bergman, R. G. *J. Am. Chem. Soc.* **1989**, *111*, 2717.

(3) Room-temperature addition of acetone to a pentane/toluene solution of $KN(SiMe_3)_2$ precipitated $KOC(CH_2)Me$, which was collected by filtration and stored at −40 °C in the drybox for up to one week without noticeable decomposition.

(4) Only a few examples of late-transition-metal O-bound enolate complexes have been reported: (a) Ito, Y.; Nakatsuka, M.; Kise, N.; Saegusa, T. *Tetrahedron Lett.* **1980**, *21*, 2873. (b) Slough, G. A.; Bergman, R. G.; Heathcock, C. H. *J. Am. Chem. Soc.* **1989**, *111*, 938. An extensive list of late-transition-metal C-bound enolate complexes is included in this reference.

(5) Reversible insertion of a chelated olefin into a metal alkyl has been observed: Flood, T. C.; Bitler, S. P. *J. Am. Chem. Soc.* **1984**, *106*, 6076. Some intermolecular additions of nucleophiles to the center of π-allyl complexes have been observed: (a) Ephritikhine, M.; Francis, B. R.; Green, M. L. H.; Mackenzie, R. E.; Smith, M. J. *J. Chem. Soc., Dalton Trans.* **1977**, 1131. (b) Periana, R. A.; Bergman, R. G. *J. Am. Chem. Soc.* **1984**, *106*, 7272.

(6) For previously reported oxametallacyclobutane complexes, see: (a) Scholdder, T.; Ibers, J. A.; Lenarda, M.; Graziani, M. *J. Am. Chem. Soc.* **1974**, *96*, 6893. (b) Lenarda, M.; Ros, R.; Traverso, O.; Pitts, W. D.; Baddley, W. H.; Graziani, M. *Inorg. Chem.* **1977**, *16*, 3178. (c) Klein, D. P.; Hayes, J. C.; Bergman, R. G. *J. Am. Chem. Soc.* **1988**, *110*, 3704. (d) Ho, S. C.; Hentges, S.; Grubbs, R. H. *Organometallics* **1988**, *7*, 780. (e) Hoover, J. F.; Stryker, J. M. *J. Am. Chem. Soc.* **1989**, *111*, 6466. For oxametallacyclobutene complexes, see: (f) Vaughan, G. A.; Hillhouse, G. L.; Lum, R. T.; Buchwald, S. L.; Rheingold, A. L. *J. Am. Chem. Soc.* **1988**, *110*, 7215. (g) Vaughan, G. A.; Sofield, C. D.; Hillhoue, G. L. *J. Am. Chem. Soc.* **1989**, *111*, 5491.

0002-7863/90/1512-3234$02.50/0